HYDROLOGICAL PROCESSES
Hydrol. Process. **18**, 2565–2578 (2004)
Published online 12 May 2004 in Wiley InterScience (www.interscience.wiley.com). DOI: 10.1002/hyp.1467

Experimental study of consolidation properties of unsaturated soils during draining

Kai-Yuan Ke,[1] Yih-Chi Tan,[1]* Chu-Hui Chen,[2] Kin-Sang Chim[1] and Tian-Chyi J. Yeh[3]

[1] *Department of Bioenvironmental Systems Engineering, and Hydrotech Research Institute, National Taiwan University, 1, Sec. 4 Roosevelt Road., Taipei 10617, Taiwan, R.O.C.*
[2] *Department of Civil Engineering, Chung-Kuo Institute of Technology, 56, Sec. 3 Hsing Lung Road., Taipei 106, Taiwan, R.O.C.*
[3] *Department of Hydrology and Water Resources, The University of Arizona, Tucson, AZ 87521-0011, USA*

Abstract:

Changes in groundwater elevation may cause a change in the net normal stress and matric potential within the soil mass, which results in volume changes of unsaturated soil. This research investigated the relationship between the drawdown of groundwater and the characteristics of volumetric compressibility of unsaturated soil. Sand column experiments were designed and conducted to measure the volume changes of coarse and fine sands under different types of drainage conditions at fast and slow drainage rates. The finite element program FEMWATER was calibrated and used to simulate the distributions of stress, tension and moisture content within the sands. Finally, based on the changes of net normal stress and matric potential and the observed volume change of the sands, a least-square method was applied to determine the volumetric consolidation parameters of the unsaturated soils. Copyright © 2004 John Wiley & Sons, Ltd.

KEY WORDS land subsidence; sand box test; unsaturated soil; compressibility

INTRODUCTION

Land subsidence is often caused by withdrawal of ground water. This withdrawal reduces the pore-water pressure and increases the intergranular stress in the solid matrix, which compacts the solid skeleton of the aquifer, and manifests itself in the form of land subsidence. Although this phenomenon is significant in confined and leaky confined aquifers, it may also occur in phreatic aquifers. In fact, changes in pore-water pressure caused by a change in saturation in the unsaturated zone can contribute significantly to the total subsidence.

Terzaghi (1936) proposed the concept of 'effective stress' to describe the consolidation process of fully saturated porous media, using a single stress-state variable. The effective stress concept was extended to unsaturated porous media using a single stress variable but considering the unsaturated medium as a three-phase system (soil particle, water and air) (Biot, 1941; Bishop, 1959; Jennings, 1961; Aitchison, 1965, 1973; Richards, 1966). Matyas and Radhakrishna (1968) and Barden *et al*. (1969) suggested the volume change of unsaturated soils be analysed in terms of two stress-state variables, i.e. the net normal stress and the matric potential. Fredlund and Morgenstern (1977) presented a theoretical stress analysis of an unsaturated soil using multiphase continuum mechanics that considers the unsaturated soil as a four-phase system, including the contractile skin (the interface between air and water) as a specific phase, in addition to water, air and solid.

A series of tests on deformable soils were conducted by Matyas and Radhakrishna (1968), Escario and Saez (1973), Cox (1978), Lloret and Alonso (1980), Maswoswe (1985) and Tadepalli *et al*. (1992) to study the relationship between the volume change and the matric potential. These tests were conducted by

* Correspondence to: Yih-Chi Tan, Department of Bioenvironmental Systems Engineering, and Hydrotech Research Institute, National Taiwan University, 1, Sec. 4 Roosevelt Road, Taipei 10617, Taiwan, R.O.C. E-mail: yctan@ccms.ntu.edu.tw

Received 7 January 2003
Accepted 1 September 2003

applying suctions to the soils. Sattler and Fredlund (1991) modelled the relationship between vertical ground movement and matric potential changes. They showed that, in the case of an open-vegetated field, increases in matric potential can result in shrinkage, whereas decreases in matric potential can result in swelling. Shuai and Fredlund (1998) formulated a model based on the equilibrium assumption, constitutive equations for unsaturated soils and the continuity requirement for the pore fluid phases. The model can be used to describe the volume-change behaviour pore-water pressure and vertical total stress development in unsaturated soil during the swelling oedometer test. Askar and Jin (2000) derived a relationship between volume changes and corresponding water losses, and modelled the effect of different shrinkage phases of a clayey soil.

Few studies have investigated the relationship between groundwater drawdown and soil volume change in terms of the net normal stress and matric potential. In this paper we conducted sand-column draining experiments to analyse the relationship between the change in volume and stress, net normal stress and matric potential in unsaturated soils.

THEORY

The characteristic of soil volume change can be expressed by the stress state of soil, which is a function of stress-state variables that are independent of the soil properties (Fung, 1977). The number of stress-state variables that can be used to describe the stress state of the soil depends on the number of phases involved. As mentioned in the introduction, a single stress-state variable is suitable for describing two-phase saturated soil systems (i.e. water and soil particles). However, when unsaturated soils involve a three-phase (soil particle, water and air) or four-phase (soil particle, water, air and contractile skin) system, two or more stress-state variables are needed to characterize the volume change property of the soil system.

Saturated soils

In this paper, 'saturated soil' means that voids in the soil are completely occupied by the water, although Rodebush and Buswell (1958) reported that there can be about 2% of dissolved air in the water because of the structure of water molecules. The dissolved air was ignored in the current study; a saturated soil–water system is assumed to be a two-phase system (soil particle and water). For saturated soils, the 'effective stress' proposed by Terzaghi (1936) is commonly accepted

$$\sigma' = \sigma - u_{\mathrm{w}} \tag{1}$$

where σ' is the effective stress ($\mathrm{M/LT^2}$), σ denotes the total stress ($\mathrm{M/LT^2}$) and u_{w} represents pore-water pressure ($\mathrm{M/LT^2}$). Effective stress is a stress-state variable that describes the volume change behaviour of saturated soils. The consolidation theory for saturated soil was derived under the following assumptions (Terzaghi, 1943): (i) the soil–water system is homogeneous; (ii) the medium is fully saturated; (iii) the compressibility of water is negligible; (iv) the compressibility of soil grains is caused by soil grain rearrangement; (v) the flow of water is one-dimensional in the direction of consolidation; (vi) Darcy's law is valid; and (vii) there is a unique linear relationship between the volume change and the effective stress. As a result, the pore-water pressure in the soil during consolidation can be described by

$$c_{\mathrm{v}} \frac{\partial^2 u_{\mathrm{w}}}{\partial z^2} = \frac{\partial u_{\mathrm{w}}}{\partial t} \tag{2}$$

in which the coefficient of consolidation ($\mathrm{L^2/T}$) is defined as $C_{\mathrm{v}} = \dfrac{k}{\gamma_{\mathrm{w}} m_{\mathrm{v}}}$ (where m_{v} is the coefficient of volumetric compresibility of saturated soil ($\mathrm{L^2/M}$), k is hydraulic conductivity (L/T) and γ_{w} is the unit weight of water ($\mathrm{M/L^3}$). A linear relation of volume change and effective stress is used to calculate the change in the soil volume

$$\frac{\mathrm{d}V}{V} = m_{\mathrm{v}} \mathrm{d}\ (\sigma - u_{\mathrm{w}}) = m_{\mathrm{v}} \mathrm{d}\sigma' \tag{3}$$

Equation (3) shows that an increase in the effective stress in soil leads to a decrease in the soil volume, and vice versa. Generally, Equation (2) is used with appropriate boundary and initial conditions to derive the solution for pore-water pressure in space and time, and then values and rates of pore-water pressure dissipation are used in Equation (3) to determine the values and rates of consolidation.

Unsaturated soils

Many researchers (Coleman, 1962; Jennings and Burland, 1962; Bishop, 1963; Burland, 1964, 1965; Blight, 1965) attempted to relate a single stress-state variable such as the effective stress to the volume change of soils under unsaturated conditions. They concluded that the relationship is neither unique nor difficult to apply to realistic situations. Thus, two stress-state variables have been introduced (Aitchison, 1967; Matyas and Radhakrishna, 1968; Barden *et al*., 1969) to investigate the change in the volume of unsaturated soils. Fredlund and Morgenstern (1977) considered unsaturated soil as a four-phase system, and proposed a stress-state variable equation with the net normal stress defined as the total stress subtracting the pore-air pressure ($\sigma - u_a$) and the matric potential ($u_a - u_w$). The matric potential is the capillary force and adsorption between soil particles and porewater. The greater the matric potential is, the lower the soil moisture.

Fredlund's theory (Fredlund and Hasan, 1979; Fredlund, 1993) assumes: (i) the air phase is continuous; (ii) the coefficients of volume change (m_{1s}, m_{2s}) for the soil remain constant during the consolidation process; (iii) the coefficients of permeability for the air and water phases are assumed to be a function of the stress state; (iv) the effect of air diffusing through water, air dissolving in water and the movement of water vapour are negligible; (v) the soil particles and the porewater are incompressible; and (vi) strains occurring during consolidation are negligible.

Based on the above assumptions, Fredlund (1979) derived the main consolidation equation for unsaturated soils:

$$\frac{dV}{V} = m_{1S}d(\sigma - u_a) + m_{2S}d(u_a - u_w) \tag{4}$$

in which m_{1s} denotes the coefficient of soil volume change with respect to a change in net normal stress and m_{2s} represents the coefficient of soil volume change with respect to a change in matric potential. When the soil is unsaturated, $m_{1s} \neq m_{2s}$; when it is fully saturated, $m_{1s} = m_{2s} = m_v$ and Equation (4) equals Equation (3).

In our experiments, lowering the water level introduced air into the sand column (see following section); we thus assume that the air phase in the column was continuous with the atmosphere (i.e. $u_a = 0$). With this assumption, Equation (4) is simplified and given as

$$\frac{dV}{V} = m_{1S}d(\sigma) + m_{2S}d(-u_w) \tag{5}$$

Equation (5) shows that the volume change of unsaturated soil is affected by both the change of total stress and the negative porewater pressure. Barden *et al*. (1969) found that a stable soil tends to swell when there is a decrease of either net normal stress or matric potential, thus m_{1s} and m_{2s} are negative values. In a collapsible or metastable soil, the consolidation is caused by the decrease of net normal stress or matric potential, and m_{1s} and m_{2s} are positive values.

SAND COLUMN EXPERIMENTS

Experimental setup

An acrylic tank 98 cm long, 28 cm wide and 80 cm high was constructed to accommodate two sand columns. Each acrylic sand column had an inner radius of 5 cm, an outer radius of 6 cm and a height of 50 cm. The circular sand columns were selected to ensure the same boundary effect from all directions to the column centre, and measurements in the column are representative. Fine and coarse sands were used. Their

grain size distribution is shown in Figure 1a. The saturated hydraulic conductivity values were determined by constant head permeability tests. Water release curves of the two sands (Figure 1b) were measured using a pressure plate device. The soils' physical and hydraulic properties are listed in Table I. Compressibility of the sands may be low but our preliminary tests suggested that a column filled with 47 cm of sand can yield measurable consolidation.

One of the columns was designed with a non-perforated sidewall to simulate the consolidation under no side-drainage scenarios. The sidewall of the other column was uniformly drilled in 735 locations to investigate consolidation under side-drainage scenarios. In addition, two acrylic bottom plates with radius of 7 cm and thickness of 1 cm were designed for the columns: one was non-perforated; the other was uniformly perforated with 30 holes to allow bottom drainage. To prevent the sand from leaking out from the perforated sidewall and bottom, a piece of filter paper lined the column. A round plate with a radius of 4·5 cm was placed on top

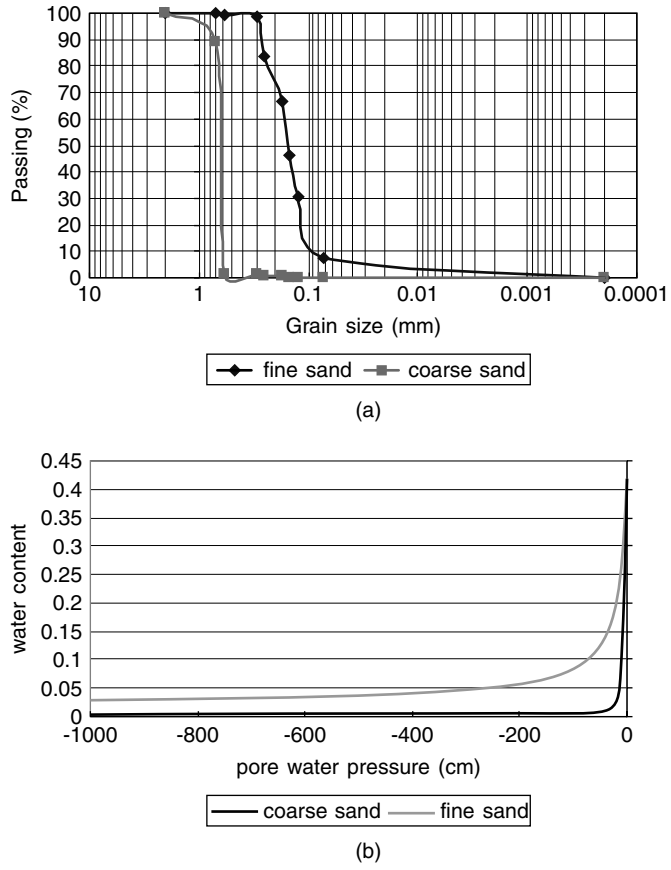

Figure 1. (a) Grain size distributions and (b) moisture release curves of the coarse and fine sand

Table I. Parameters of soil in laboratory test

	G_S	n	K_S(cm/s)	m_v(m^2/N)	α	β	θr	θs
Coarse sand	2·62	0·338	$4{\cdot}17 \times 10^{-3}$	$2{\cdot}7 \times 10^{-9}$	0·183	2·96	0·0018	0·34
Fine sand	2·60	0·417	$3{\cdot}33 \times 10^{-3}$	$9{\cdot}3 \times 10^{-9}$	0·110	1·70	0·028	0·417

of the sand in each column, and a dial gauge was set on the cap to ensure that the measurements represented the average over the cross-section area of the column.

The tank with the sand columns was filled with water to a desired height and then a pump was used at two different rates to lower the water level in the tank. The fast drainage rate lowered the water level by 50 cm over 110 min and the slow drainage rate took 220 min. Figure 2 is a schematic illustration of the experimental setup.

Drainage consolidation experiments

In addition to the two drainage rates, three drainage scenarios representing one- and multidimensional flow fields were investigated: (i) side drainage (SD); (ii) bottom drainage (BD); and (iii) both side and bottom drainage, also called all-drainage (AD). The combination of the two drainage rates, three drainage scenarios and two different sands led to 12 experiments (Table II).

Several preliminary tests were performed to optimize experimental procedures, to check packing procedures and to ensure accuracy of measurements. During one preliminary test, the fine sand with the AD scenario at the slow drainage rate was used. The following is the procedure for our drainage consolidation experiments.

1. Prepare the sand column as one of the three drainage scenarios in the water tank and choose the type of sand for testing.
2. Pack the sand in the column in five steps; for the coarse sand column, 320 g were used in each step whereas 280 g were used for the fine sand column. At the completion of each step, the column was tapped carefully to ensure uniform settlement.
3. Lower the sand column into the water tank, and install the dial gauge.
4. Fill the tank to a water level that is equal to the height of the top of the sand column.
5. Wait until the sand is fully saturated (about 1 h for the coarse sand, 2 h for the fine sand).
6. When the soil is fully saturated, select one of the two pump rates to lower the water level in the tank.
7. Record the dial gauge reading every 5 min until the water level reaches the bottom of the sand column.

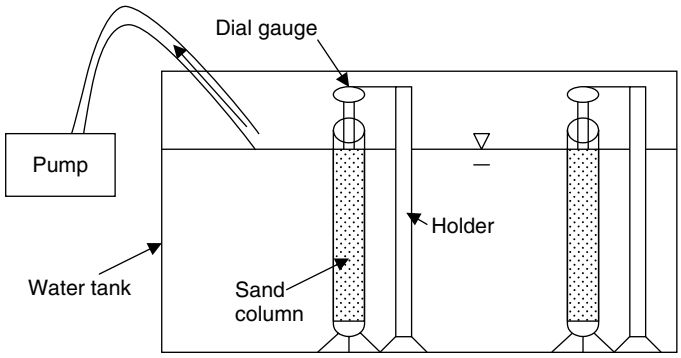

Figure 2. The design of the consolidation drainage experiments

Table II. Combination of sand-column pumping test

	All drainage (AD)	Side drainage (SD)	Bottom drainage (BD)
Coarse sand, quick pumping	CQAD	CQSD	CQBD
Coarse sand, slow pumping	CSAD	CSSD	CSBD
Fine sand, quick pumping	FQAD	FQSD	FQBD
Fine sand, slow pumping	FSAD	FSSD	FSBD

Because the dial gauge was laid on the top of the soil column and our tensiometer had to be inserted from the top of the soil to measure the porewater pressure, the above experiments were repeated with a tensiometer inserted from the top to a depth of 4·5 cm, without the dial gauge. The voltage from the tensiometer's transducer was recorded by a datalogger (converted to pressure) at a 5-min interval.

After each drainage consolidation experiment, the 47 cm height sand column was removed from the tank and sliced into nine pieces (5 cm high per piece from the bottom, and discarding the top 2 cm) to measure the water content of the nine sections of sand column. The water contents were used for model calibration, and will be discussed in the analysis section. The nine slices were numbered from 1 to 9 from the bottom to the top.

Experimental results

Figure 3 illustrates a typical result of the drainage consolidation experiments. It shows the volume change of the coarse sand for three different drainage scenarios (AD, SD and BD) with the slow drainage rate. In all the scenarios, the sand consolidated early in the experiment, the consolidation stopped at an intermediate time, and the soil swelled during the final phase of drainage. The maximum consolidation (MC) and the rate to maximum consolidation (RTMC), i.e. the ratio of the maximum consolidation to the time to the MC, are shown in Figure 4a and b. The MC is 0·141 mm for the coarse sand with the slow drainage rate, which is very close in value to the MC for the SD condition, which was 0·132 mm. The BD has the lowest MC value, 0·078 mm. The AD and SD conditions also have higher RTMC than BD.

The experiments also showed that the MC values of CSAD and CSSD are about 0·06 mm greater than CSBD and the MC values of FSAD and FSSD are 0·03 mm greater than FSBD. Therefore, under the slow drainage rate, different types of drainage (or flow fields) had an influence on the MC values in both the coarse and fine sands. In particular, multidimensional flow conditions produced greater consolidation than one-dimensional flow. Moreover, the difference of the MC values between the coarse sand and the fine sand is 0·042 mm for AD, 0·05 mm for SD and 0·016 mm for BD, indicating that particle size affects the MC value. In addition, the coarse sand had higher RTMC values than the fine sand, regardless of the type of drainage. Higher RTMC values were also observed in the experiments with the fast drainage rate. The higher RTMC values may be explained by the fact that the pore radii are larger in the coarse sand, yielding smaller capillary forces, which allow rapid variation of internal stress of the soil body and contribute to the rearrangement of soil particles. Consequently, the consolidation of the coarse sand is greater, compared with the consolidation of fine sand under all drainage conditions.

In the experiments with the fast drainage rate, the MC and RTMC values of the coarse sand were greater than those with the slow drainage rate for all three drainage scenarios. The fast draining rate led to a rapid

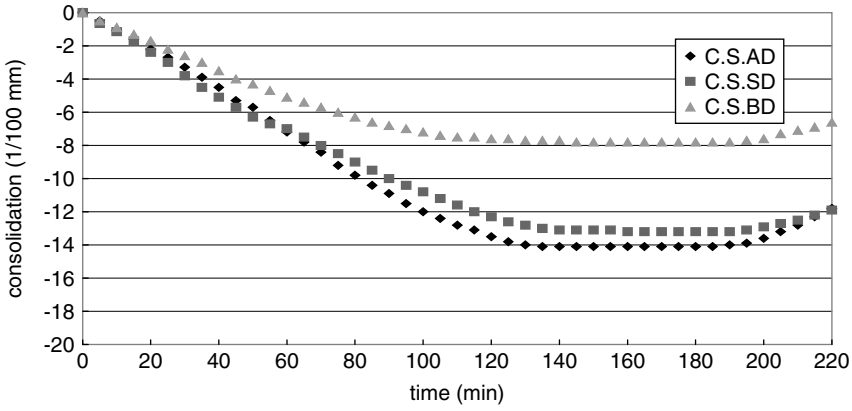

Figure 3. Comparison of volume change of CSSD, CSBD and CSAD

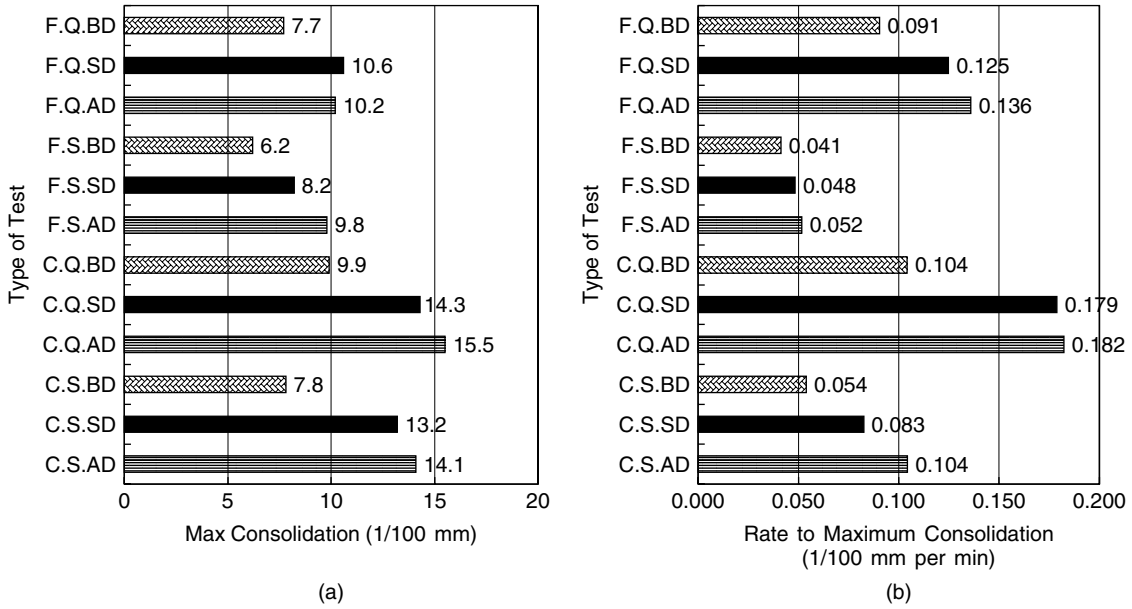

Figure 4. Comparison of (a) maximum consolidation and (b) rate to maximum consolidation of different types of consolidation drainage experiments

change in the boundary condition of the soil–water system and hence accelerated the change of porewater pressure and water content of the sand. Under this circumstance, rearrangement of soil particles was enhanced, and the consolidation was more pronounced. However, the difference in the MC values caused by different drainage rates is less than 0·02 mm, comparatively smaller than the consolidation caused by the different drainage scenarios. We conclude that the method of column drainage (or dimensionality of the flow field) is a more influential factor than the drainage rate.

The measurements of porewater pressure in the sands during all the experiments are shown in Figure 5a and b for the slow and the fast drainage rates. The porewater pressures at the measuring points were initially positive, indicative of saturation of the soils in the columns. After drainage took place, the porewater pressure in the coarse sand reached a stable value at approximately 130 min during the slow drainage rate, and 60 min during the fast drainage rate. The porewater pressures in the fine sand never approached stable values during the experiments. These results merely reflect the effect of differences in grain-size/pore-size distribution between the coarse and fine sands (Figure 1a) (in turn, water retention curve, Figure 1b). Because of the highly uniform pore-size distribution of the coarse sand, once large pores are drained, water remains in the small pores as residual water content retained by a constant capillary pressure. Conversely, the fine sand has a broad grain size distribution, and the porewater never reaches an equilibrium condition. The different drainage scenarios also produced the similar behaviours and porewater pressure values.

In Figure 6a and b, the final water content is about 0·05 for the slices with number greater than 5 of the coarse sand column. Conversely, the water content in the fine sand did not reach any stable value.

ANALYSIS

Determination of coefficients, m_{1s} and m_{2s}, in Equation (4) requires knowledge of the porewater pressure distribution and the total stress, i.e. the sum of the water content and the weight of the sands. To determine the porewater pressure and water content profiles in the columns under different drainage conditions, we used the finite element program FEMWATER (Yeh and Ward, 1996).

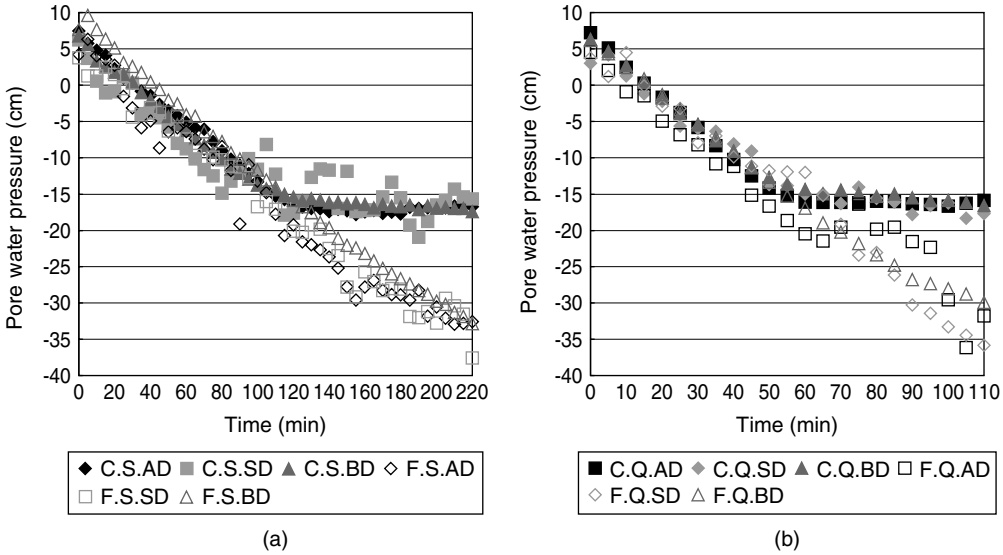

Figure 5. Porewater pressure of coarse and fine sand measured at 4·5 cm below the top of the sand column during (a) slow and (b) fast drainage

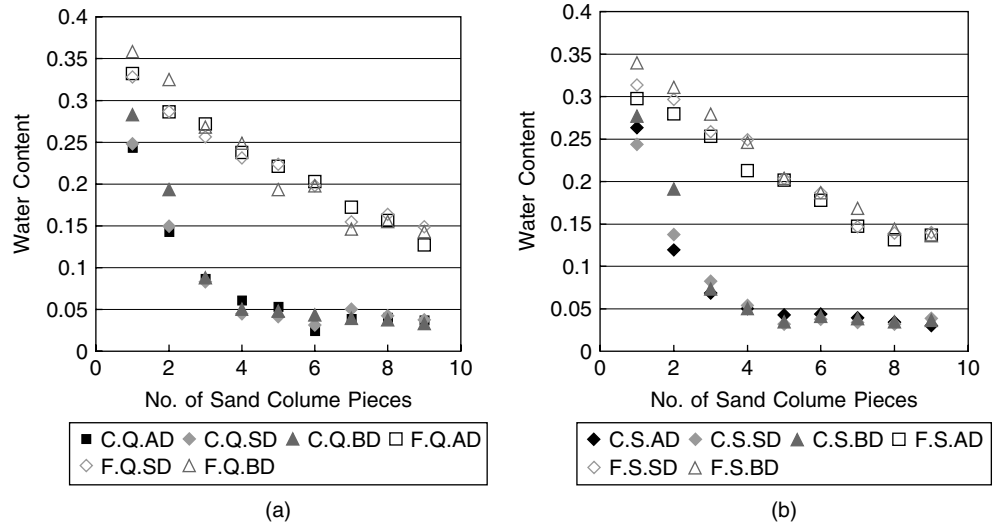

Figure 6. Distribution of water content in the coarse and fine sand columns during (a) the slow drainage at 220 min and (b) the fast drainage at 110 min

The governing equation solved by FEMWATER is the Richards equation

$$\frac{\mathrm{d}\theta}{\mathrm{d}h}\frac{\partial h}{\partial t} = \nabla\{k(h)[\nabla h + \nabla Z]\} \tag{6}$$

where h denotes the pressure head (L), t is time (T), Z is the elevation head (L), θ is the water content (L^3/L^3) and $K(h)$ is the hydraulic conductivity (L/T), which is a function of h under unsaturated conditions. The relationship between water content and pressure head and hydraulic conductivity were assumed to follow

the van Genuchten (1980) equations

$$K_r = \frac{K(\theta)}{K_s} = \theta_e^{0.5}\left[1 - (1 - \theta_e^{\frac{1}{\gamma}})^{\gamma}\right]^2 \tag{7}$$

$$\theta_e = [1 + (\alpha h)\beta]^{-\gamma} = \frac{\theta - \theta_r}{\theta_s - \theta_r} \quad \text{for} \quad h < 0 \tag{8}$$

$$\theta_e = 1 \qquad \text{for} \quad h \geq 0 \tag{9}$$

The relative hydraulic conductivity (dimensionless) is denoted by K_r, $K(\theta)$ is the hydraulic conductivity (L/T), K_s denotes the saturated conductivity (L/T), θ_e is the effective saturation (dimensionless), θ_s is the saturated water content (dimensionless), θ_r represents the residual water content (dimensionless), α (1/L), β (dimensionless) and γ (dimensionless) are parameters with values that depend on the soil's properties, and $\gamma = 1 - 1/\beta$. The hydraulic conductivity is assumed to be homogeneous and isotropic. Parameters of the water release curves (α, β, θ_s, and θ_r) listed in Table I were used for the simulation. It is likely that during consolidation, these functional relations may change, but they were assumed constant during our investigation.

To simulate the evolution of pressure and moisture profiles in the sand column, a solution domain representing a quarter of a cylinder was used; we assumed axis symmetry in the columns. The domain is 47 cm in height, and was discretized into 30 elements in the vertical direction. Each element is automatically divided into 97 triangular elements by FEMWATER, resulting in a total of 1922 nodes and 2910 elements. The top of the simulation domain was assumed to be a no flow boundary. Prescribed head conditions were used at the bottom for the AD and BD experiments, whereas a no flux boundary was used for the SD experiment. The prescribed head conditions were set equal to the observed water level in the tank, which varied with time. The two converging sides of the domain were assumed to be no flow. The other side boundary was assigned as a prescribed head and flux boundary (i.e. a time-varying hydrostatic condition for the portion below the water level and a no flow boundary condition above the water level) for the AD and SD experiments, and a no flux boundary for the BD experiment. A hydrostatic pressure distribution was used to represent the initial condition of the experiments.

Model calibration was performed to adjust K_s values, and the other parameters were assumed constant as listed in Table I, as the impact of the other parameters is believed to be negligible. We adjusted the K_s in the model until the simulated porewater pressure and water content were comparable to the measured values in the BD experiment. The calibrated K_s value was used to simulate the distribution of u_w and θ under SD and AD. The steps were repeated until the simulated and observed pressure and water content were in reasonable agreement.

Figure 7 shows the observations of u_w in the CSBD, FSBD, CQBD and FQBD experiments, as well as the simulated values obtained using three different K_s values, including the laboratory measured value and two calibrated values. The calibrated K_s values, $4{\cdot}17 \times 10^{-2}$ cm/s for coarse sand and $3{\cdot}33 \times 10^{-2}$ cm/s for fine sand, produced better agreement with the observed u_w than the laboratory measured values ($4{\cdot}17 \times 10^{-3}$ cm/s and $3{\cdot}33 \times 10^{-3}$ cm/s for coarse and fine sand, respectively.) Although the difference between the simulated and measured values is an order of magnitude, we used the calibrated ones for our simulations because they reproduce the observed pressure, which is the focus of the analysis. The measured θ data and the data simulated using the calibrated K_s values for CSBD and FSBD experiments (Figure 8) show reasonable agreement for soil slices numbered 4 to 9. For soil slices numbered 1 to 3 (namely, the bottom three slices), the measured values of θ were smaller than the simulated values. This may be attributed to water loss from the soil pieces when the soil slices were taken out for measurement. This phenomenon is more pronounced in the bottom soil slices, because they were essentially saturated and thus water likely leaked out when the measurement took place. Notice that there is a higher difference between measured value and the simulated in coarse sand

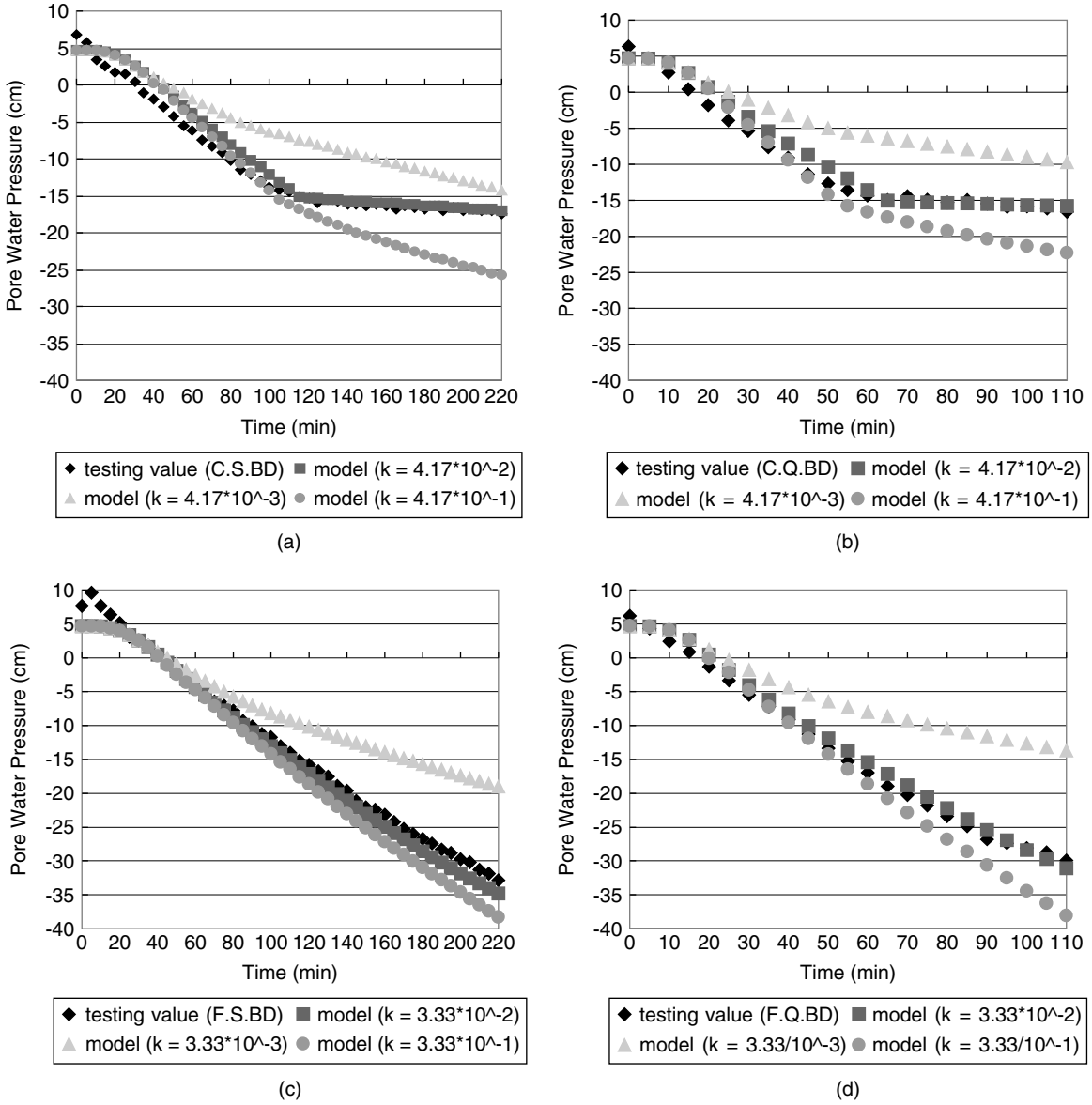

Figure 7. Comparison of simulated and observed porewater pressures of (a) CSBD, (b) CQBD, (c) FSBD and (d) FQBD (unit of k is cm/s)

than fine sand. This probably confirms the leakage explanation because the coarse sand has fewer capillaries than the fine sand.

Using the simulated water content distribution and specific gravity of the sands (Table I), the total stress over the column at different times was calculated by

$$\sigma(t) = \frac{(W_s + W_w)}{A} = \frac{(G_s \rho_w V_s + \theta V \rho_w) g}{A} \tag{10}$$

where W_s is the weight of soil particles, W_w denotes the weight of water in the sand, G_s represents the specific gravity of soil particle, equal to ρ_s/ρ_w, ρ_s and ρ_w are the density of solid and water, respectively, g

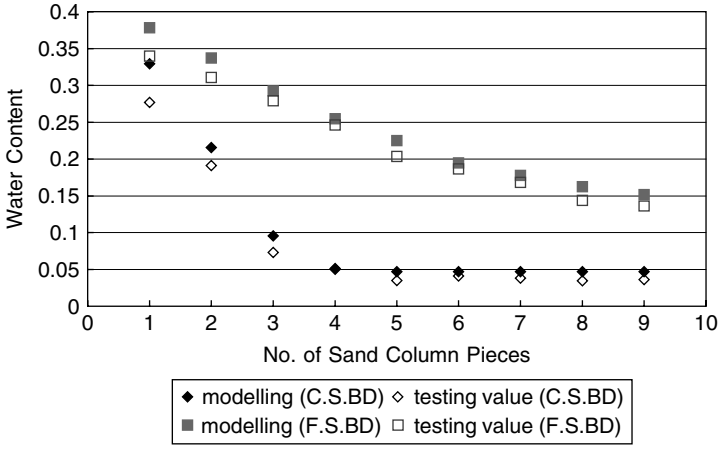

Figure 8. Comparison of observed and simulated θ for CSBD and FSBD at 220 min with the calibarated K_s values

is the gravitational acceleration, V_s and V are the volume of solids, and the total volume of sand, and A is the unit area of the soil column. Using the measured change in volumes, the porewater pressures averaged over the column and the total stresses over the experimental time periods, regression analyses were conducted to determine the coefficients of volume change m_{1s} and m_{2s}. The analyses were based on Equation (4), i.e. the difference between the observed and calculated changes in soil volumes was minimized.

For the drainage consolidation experiments, the consolidation measured by the dial gauge represents the summation of saturated consolidation below the water table and the unsaturated consolidation above the water table. To evaluate the coefficient of soil volume change, consolidation caused by the saturated zone was ignored. The laboratory measurements of consolidation from the saturated zone range from 10^{-3} to 10^{-4} mm (Table I). These values are negligible compared with the experiment observations of 10^{-2} mm; the volumetric change caused by the saturated zone thus is neglected. Hence the consolidation is assumed to be mainly caused by the unsaturated portion of the sand column.

The coefficients of volume change m_{1s} and m_{2s} for all the experiments are listed in Table III. As the coefficient of volume change, generally speaking, is a soil property independent of the drainage rate or drainage condition, values were averaged using the coefficients for the same type of sand determined from the two drainage rates and three drainage scenarios. The average values for m_{1s} were found to be $1{\cdot}87 \times 10^{-4}$ m^2/N and $1{\cdot}47 \times 10^{-4}$ m^2/N for coarse and fine sand, respectively. The average values for m_{2s} were $3{\cdot}39 \times 10^{-6}$ m^2/N and $1{\cdot}08 \times 10^{-6}$ m^2/N for the coarse and fine sand, respectively. The variation of these four coefficients is less than 20%, suggesting that these averaged coefficients are independent of the drainage rate and condition.

All the values for m_{1s} and m_{2s} were found to be positive, indicating that unstable structure of the sands existed when the sand columns were created. Based on the m_{1s} and m_{2s} values and simulated porewater pressure and moisture content profiles, changes can be evaluated in the consolidation rate caused by either the net normal stress or the matric potential. In general, during the drainage experiments, the net normal stress that compresses soils decreased, and the matric potential (that makes soils swell) increases. Using the FSSD experiment as an example, Figure 9 illustrates the consolidation and swelling rates as a function of time. Both rates were about the same at the beginning, indicating that the changing volume in the beginning stage is not obvious (note that the consolidation rate should be negative, but we take it as positive for easy comparison with the swelling rate). After about 30 min, the consolidation rate gradually exceeded the swelling rate, and the consolidation became more apparent. At later times, both the swelling rate and consolidation rate declined. However, the swelling rate declined slower than the consolidation rate, and finally the soil began to swell.

Table III. Estimated coefficient of soil volume change

Coarse sand	$m_{1s}(m^2/N)$	$m_{2s}(m^2/N)$	Fine sand	$m_{1s}(m^2/N)$	$m_{2s}(m^2/N)$
CQAD	$2{\cdot}16 \times 10^{-4}$	$3{\cdot}95 \times 10^{-6}$	FQAD	$1{\cdot}84 \times 10^{-4}$	$1{\cdot}38 \times 10^{-6}$
CSAD	$2{\cdot}07 \times 10^{-4}$	$3{\cdot}70 \times 10^{-6}$	FSAD	$1{\cdot}22 \times 10^{-4}$	$0{\cdot}85 \times 10^{-6}$
CQSD	$1{\cdot}89 \times 10^{-4}$	$3{\cdot}44 \times 10^{-6}$	FQSD	$1{\cdot}65 \times 10^{-4}$	$1{\cdot}21 \times 10^{-6}$
CSSD	$1{\cdot}84 \times 10^{-4}$	$3{\cdot}26 \times 10^{-6}$	FSSD	$1{\cdot}36 \times 10^{-4}$	$0{\cdot}98 \times 10^{-6}$
CQBD	$1{\cdot}73 \times 10^{-4}$	$3{\cdot}21 \times 10^{-6}$	FQBD	$1{\cdot}50 \times 10^{-4}$	$1{\cdot}13 \times 10^{-6}$
CSBD	$1{\cdot}52 \times 10^{-4}$	$2{\cdot}77 \times 10^{-6}$	FSBD	$1{\cdot}23 \times 10^{-4}$	$0{\cdot}91 \times 10^{-6}$
Average	$1{\cdot}87 \times 10^{-4}$	$3{\cdot}39 \times 10^{-6}$	Average	$1{\cdot}47 \times 10^{-4}$	$1{\cdot}08 \times 10^{-6}$
Variation	0·1243	0·1210	Variation	0·1676	0·1866

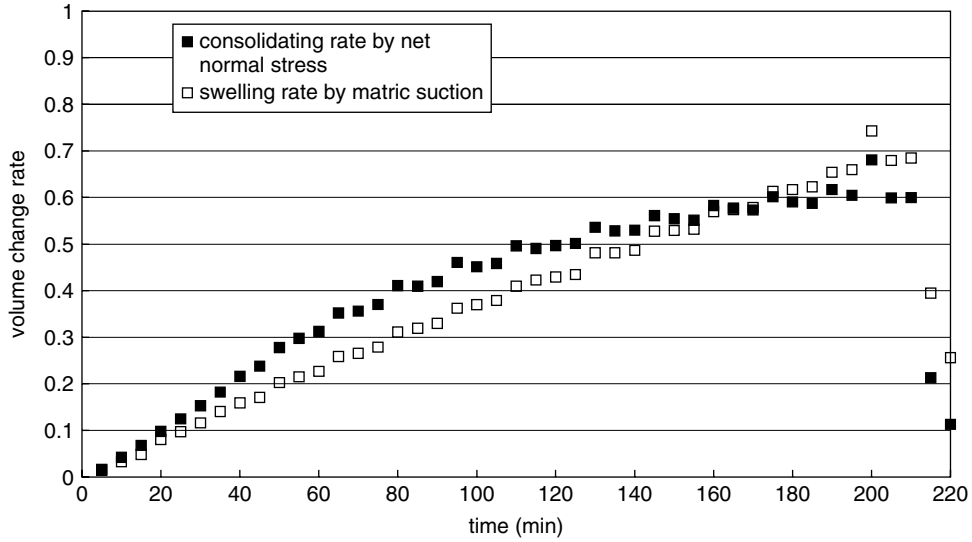

Figure 9. Comparison of volume change rates of FSSD caused by net normal stress and matric suction during the slow drainage experiment

This explains the observations that in all the scenarios, the sand consolidated early in the experiment, the consolidation stopped at an intermediate time, and the soil swelled during the final phase of drainage.

Table III shows that for the fast drainage scenario, m_{1s} and m_{2s} of AD and SD are greater than those of BD; for the slow drainage scenario, the values for both AD and SD are generally greater than BD. Such a general trend appears to indicate dependence of the values on the dimensionality of the flow. That is, multidimensional flow scenarios tend to yield larger m_{1s} and m_{2s} values than one-dimensional flow scenarios.

We also compared the observed consolidation with calculations that used the regressed m_{1s} and m_{2s} values and the averaged values for the coarse and fine sand under the side drainage scenario (Figure 10). For the fine sand, the behaviours of the calculated consolidation using either the regressed values or the averaged values are consistent with the observed: the sand consolidates at an initial stage and swells later. For coarse sand, however, the calculated consolidation curves show that the sand swells a little at first, then consolidates and resumes swelling.

CONCLUSIONS

By comparing the consolidation that resulted from different drainage scenarios, we conclude that the value and rate of consolidation are about the same for both conditions of all-drainage and side drainage, and both are

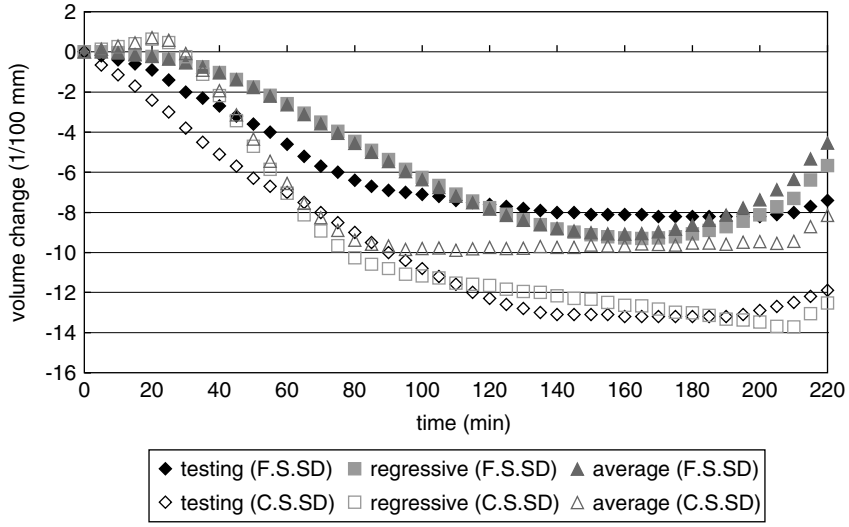

Figure 10. Comparison of observations with calculated consolidation (using regressed and average coefficients) of the coarse and the fine sand during the slow drainage under the SD condition

greater than the bottom-drainage scenario. By comparing the effects of different drainage rates, we conclude that fast drainage will result in a greater consolidation than a slow drainage. These two phenomena are explained by the rapid change of the boundary condition that results in rapid variation of stress inside the soil body. Thus, the soil is easier to compress. Results of running the experiments with different particle sizes indicate that coarse sand is more compressible than fine sand, because the pore size of coarse sand is greater than the fine sand. In other words, smaller capillary forces and a faster drainage rate will result in faster rearrangement of soil particles of the coarse sand.

ACKNOWLEDGEMENTS

This study was supported by the National Science Council of Taiwan under contract NSC-90-2313-B-002-324. The last author was funded in part by NSF and SERDP of USA by a grant EAR-0229717. The authors are also grateful for the contributions of Dr Chen-Wuing Liu, Cheng-Haw Lee and Jet-Chau Wen. Appreciation is also extended to Martha P.L. Whitaker, for technical editing of this document.

REFERENCES

Aitchison GD. 1965. Soil properties, shear strength, and consolidation. In *Proceedings of the 6th International Conference on Soil Mechanics and Foundation and Engineering*, Montreal, canada **3**: 318–321.

Aitchison GD. 1967. Separate roles of site investigation. Quantification of soil properties, and selection of operational environment in the determination of foundation design on expansive soils. *Proceedings of the Third Asian Regional Conference on Soil Mechanics and Foundation Engineering*, Haifa, Israel.

Aitchison GD. 1973. The quantitative description of the stress deformation behavior of expansive soils—preface to set of papers. In *Proceedings of the 3rd International Conference on Expansive Soils*, Haifa, Israel **2**: 79–82.

Askar A, Jin Y-C. 2000. Macroporous drainage of unsaturated swelling soil. *Water Resources Research* **36**(5): 1189–1197.

Barden L, Madedor AO, Sides GR. 1969. Volume change characteristics of unsaturated clay. *Journal of the Soil Mechanics and Foundations Division, American Society of Civil Engineers* **95**(SM1): 33–52.

Biot MA. 1941. General theory of three-dimensional consolidation. *Journal of Applied Physics* **12**(2): 155–164.

Bishop AW. 1959. The principle of effective stress. *Teknisk Ukeblad* **106**(39): 859–863.

Bishop AW. 1963. Some aspects of effective stress in saturated and unsaturated soils. *Geotechnique* **13**: 177–197.

Blight GE. 1965. A study of effective stresses for volume change. In *Moisture Equilibrium and Moisture Changes in Soils Beneath Covered Areas*. Butterworths: Sydney; 259–269.

Burland JB. 1964. Effective stresses in partly saturated soils. Discussion of 'Some aspects of effective stress in saturated and partly saturated soils' by Blight GE Bishop AW. *Geotechnique* **14**: 65–68.
Burland JB. 1965. Some aspects of the mechanical behavior of partly saturated soils. In *Moisture Equilibrium and Moisture Changes in Soils Beneath Covered Areas*. Butterworths: Sydney; 270–278.
Coleman JD. 1962. Stress/strain relations for partly saturated soils. *Geotechnique* **12**(4): 348–350.
Cox DW. 1978. Volume change of compacted clay till. In *Proceedings of the International Civil Engineering Conference on Clay Tills*; 79–86.
Escario V, Saez J. 1973. Measurement of the properties of swelling and collapsing soils under controlled suction. In *Proceedings of the 3rd International Conference on Expansive Soils*, Haifa, Israel **1**: 195–200.
Fredlund DG. 1993. *Soil Mechanics for Unsaturated Soils*. Wiley: New York.
Fredlund DG, Hasan JU. 1979. One-dimensional consolidation theory: unsaturated soils. *Canadian Geotechnical Journal* **16**(3): 521–531.
Fredlund DG, Morgenstern NR. 1977. Stress-state variables for unsaturated soils. *Journal of the Geotechnical Engineering Division, American Society of Civil Engineers* **103**(GT5): 447–466.
Fung YC. 1977. *A First Course in Continuum Mechanics*, 2nd edn. Prentice-Hall: Englewood Cliffs, NJ.
Jennings JE. 1961. A revised effective stress law for use in the prediction of the behavior of unsaturated soils. In *Pore Pressure and Suction in Soils*, Conference Organized by the British National Society of International Society Soil Mechanics and Foundation Engineering at the Institute of Civil Engineers, London. Butterworths: London; 26–30.
Jennings JE, Burland JB. 1962. Limitations to the use of effective stresses in partly saturated soils. *Geotechnique* **12**(2): 432–448.
Lloret A, Alonso EE. 1980. State surfaces for partially saturated soils. In *Proceedings, 11th International Conference on Soil Mechanics and Foundation Engineering*, San francisco, CA, USA **2**: 557–562.
Maswoswe J. 1985. *Stress paths for a compacted soil during collapse due to wetting*. PhD dissertation, Imperial College, London.
Matyas EL, Radhakrishna HS. 1968. Volume change characteristics of partially saturated soils. *Geotechnique* **18**(4): 432–448.
Richards BG. 1966. The significance of moisture flow and equilibria in unsaturated soils in relation to the design of engineering structures built on shallow foundations in australia. Presented at the *Symposium On Permeability and Capillary*, American Society of Testing Materials, Atlantic City, NJ.
Rodebush WH, Buswell AM. 1958. *Properties of Water Substances*. Special Report No. 40, Highway Research Board.
Sattler PJ, Fredlund DG. 1991. Numerical modeling of vertical ground movements in expansive soils. *Canadian Geotechnical Journal* **28**: 189–199.
Shuai F, Fredlund DG. 1998. Model for the simulation of swelling-pressure measurements on expansive soils. *Canadian Geotechnical Journal* **35**: 96–114.
Tadepalli R, Rahardjo H, Fredlund DG. 1992. Measurements of matric suction and volume changes during inundation of collapsible soil. *Geotechnical Testing Journal* **15**: 115–122.
Terzaghi K. 1936. The shear resistance of saturated soils. In *Proceedings, 1st International Conference on Soil Mechanics and Foundation Engineering*, Cambridge, MA, Vol. 1; 54–56.
Terzaghi K. 1943. *Theoretical Soil Mechanics*, John Wiley: New York, USA; 270–296.
Van Genuchten MTh. 1980. A closed-form equation for predicting the hydraulic conductivity of unsaturated soils. *Soil Science Society of America Journal* **44**(5): 892–898.
Yeh GT, Ward DS. 1996. *FEMWATER: a Finite-element Model of Water Flow Through saturated—Unsaturated Porous Media.* Oak Ridge National Laboratory: Oak Ridge, TN.

